MOLECULAR AND CELLULAR BIOLOGY, Apr. 2005, p. 2846–2852 Vol. 25, No. 7
0270-7306/05/$08.00+0 doi:10.1128/MCB.25.7.2846–2852.2005

Normal Thyroid Structure and Function in Rhophilin 2-Deficient Mice

Jens Behrends,[1]†‡ Serge Clément,[1]† Bernard Pajak,[2] Viviane Pohl,[1] Carine Maenhaut,[1] Jacques E. Dumont,[1] and Stéphane Schurmans[1]*

Institut de Recherches Interdisciplinaires en Biologie Humaine et Moléculaire, Faculté de Médecine,[1] and Laboratoire de Physiologie Animale, Faculté des Sciences,[2] Institut de Biologie et de Médecine Moléculaires, Université Libre de Bruxelles, Gosselies, Belgium

Received 23 July 2004/Returned for modification 24 August 2004/Accepted 15 December 2004

Rhophilin 2 is a Rho GTPase binding protein initially isolated by differential screening of a chronically thyrotropin (TSH)-stimulated dog thyroid cDNA library. In thyroid cell culture, expression of rhophilin 2 mRNA and protein is enhanced following TSH stimulation of the cyclic AMP (cAMP) transduction cascade. Yeast two-hybrid screening and coimmunoprecipitation have revealed that the GTP-bound form of RhoB and components of the cytoskeleton are protein partners of rhophilin 2. These results led us to suggest that rhophilin 2 could play an important role downstream of RhoB in the control of endocytosis during the thyroid secretory process which follows stimulation of the TSH/cAMP pathway. To validate this hypothesis, we generated rhophilin 2-deficient mice and analyzed their thyroid structure and function. Mice lacking rhophilin 2 develop normally, have normal life spans, and are fertile. They have no visible goiter and no obvious clinical signs of hyper- or hypothyroidism. The morphology of thyroid cells and follicles in these mice were normal, as were the different biological tests performed to investigate thyroid function. Our results indicate that rhophilin 2 does not play an essential role in thyroid physiology.

Thyrotropin (TSH) is the main physiological agent regulating the thyroid gland. TSH binds to its specific receptor on the surface of the thyrocyte and activates a G protein-coupled mechanism to stimulate adenylate cyclase, leading to cyclic AMP (cAMP) production. TSH and cAMP promote thyroid cell proliferation, function, and differentiation, while the mitogenic pathway elicited by epidermal growth factor and tumor-promoting phorbol ester are associated with the loss of expression of the differentiation-specific genes (4, 5). Many of the regulatory steps of these pathways have been analyzed by means of an in vitro dog thyroid cell culture model in our laboratory in recent years (13). However, several steps of the TSH-cAMP cascade are still unknown: the molecular mechanisms of this pathway downstream of cAMP, cAMP-dependent protein kinase, and its phosphorylated targets are unclear (3).

A study aimed at the identification of genes that are positively or negatively regulated by TSH and cAMP in dog thyroid cells was thus initiated: a cDNA library was prepared from dogs treated in vivo with methimazole and propylthiouracil, two agents known to inhibit thyroid hormone synthesis (17). This inhibition leads to relief of the inhibitory control of these thyroid hormones on the hypophysis and to TSH secretion and chronic TSH stimulation of the thyroid cells. By differential screening of this cDNA library with digoxigenin-labeled cDNA probes derived from quiescent or stimulated thyroid tissues, several new differentially expressed genes were identified. Among these, rhophilin 2 (*Rhpn2*, previously reported as clone 45, p76^{RBE}, or Rho binding protein 2) was particularly well analyzed in our laboratory. *Rhpn2*, whose mRNA and protein expression is enhanced in thyrocytes following TSH stimulation of the cAMP transduction cascade in vitro (8), presents important similarities with rhophilin and contains several protein-protein interaction motifs, like HR1 and PDZ motifs, as well as a potential PDZ binding motif (8, 10). Yeast two-hybrid screening and coimmunoprecipitation experiments have recently revealed that rhophilin 2 binds specifically to the GTP-bound form of the small GTPase RhoB and to components of the cytoskeleton (8). Based on these results, it was suggested that Rhpn2 could play a key role between RhoB and potential downstream elements in the control of intracellular motile phenomena, such as the endocytosis which is involved in the thyroid secretory process following stimulation of the TSH/cAMP pathway (8).

Here, we report the production of *Rhpn2*-deficient mice and the analysis of their thyroid structure and function. We have found that mice lacking *Rhpn2* develop normally, are fertile, and have no histological, clinical, or biological signs of thyroid dysfunction. Thus, our results indicate that *Rhpn2* is dispensable for normal thyroid function and development.

MATERIALS AND METHODS

Mouse cDNA library screening. A mouse brain cDNA library in Lambda gt10 (Clontech, Palo Alto, Calif.) was screened using a heat-denatured [α-^{32}P]dATP-radiolabeled 2.2-kb dog rhophilin 2 cDNA fragment containing the complete coding region (17). Hybridization was performed at 42°C in 40% formamide, 5 mM EDTA, 6× SSC, and 0.25% nonfat dry milk for 12 h, and the final wash was carried out with 1× SSC and 0.1% sodium dodecyl sulfate at 60°C. The positive clones were sequenced on an Applied Biosystems model 377 sequencer.

5′ RACE. The rapid amplification of 5′ cDNA ends (5′ RACE) system (version 2.0) kit (Life Technologies, Gaithersburg, Md.) was used to synthetize the first-strand cDNA from mouse brain RNA by use of GSP1 primer (5′-CAT CAT TTT GAC CAG CAC ACT-3′, located in exon 8 as GSP2 and GSP3 primers) (Fig. 1A), for reverse transcription, followed by ligation of the 5′-anchor adapter. Two rounds of PCR were then performed using the nested primers GSP2 (5′-GTG AGT GAA GGT CTC TTT CAG-3′) and GSP3 (5′-AAC CCC TGC AGC TCT

* Corresponding author. Mailing address: IRIBHM, IBMM, rue des Professeurs Jeener et Brachet 12, 6041-Gosselies, Belgium. Phone: 32 2 6509825. Fax: 32 2 6509820. E-mail: sschurma@ulb.ac.be.

† J.B. and S.C. contributed equally to this work.

‡ Present address: Medizinische Hochschule Hannover, Department of Gastroenterology, Hepatology and Endocrinology, 30623 Hannover, Germany.

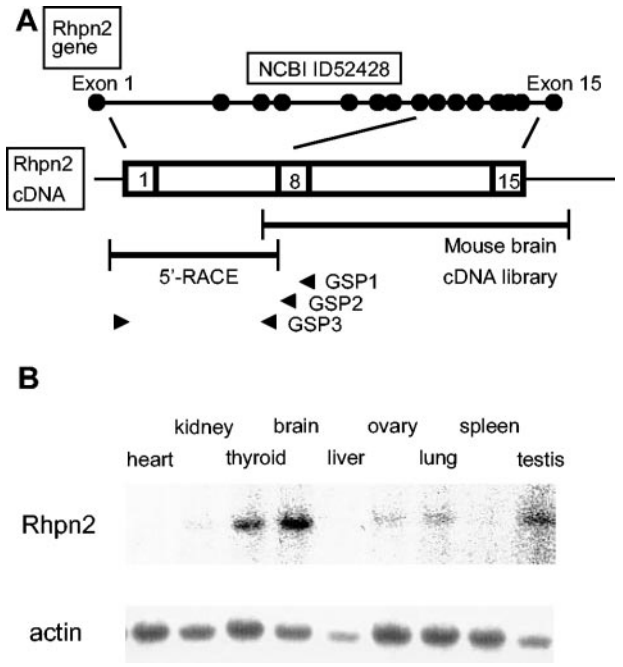

FIG. 1. Mouse rhophilin 2 gene structure, cDNA, and expression in tissues. (A) Schematic representation of the exon-intron structure of the mouse rhophilin 2 gene on chromosome 7, as reported in NCBI databases (see above). The two DNA fragments isolated by screening of a mouse brain cDNA library and by 5′ RACE are depicted as well as the three specific primers (GSP1, GSP2, and GSP3, all located in exon 8 [arrowheads]) used in 5′ RACE (see below). (B) Hybridization analysis of RNA isolated from mouse tissues with a rhophilin 2 probe or an actin probe.

TTG AAA-3′) with the 5′-anchor primer, according to the manufacturer's instructions. The unique PCR product was subcloned in PCR2 vector and sequenced as described above.

Generation of *Rhpn2* knockout mice. An 8-kb BamHI genomic DNA fragment containing exon 7 of the murine *Rhpn2* gene was cloned from a 129/Sv genomic phage library. A targeting vector was constructed by replacing a 1-kb Eco47III genomic DNA fragment which comprises the last 28 nucleotides of exon 7 and ~1 kb of the following intron by a neomycin resistance cassette (Neo). Transfection of R1 embryonic stem cells and production of chimeric mice were done using standard procedures as described previously (12). Experimental mice were 2 to 6 months old, of both sexes, and of a mixed (129/Sv × CD1) genetic background after two to five backcrosses with CD1 mice. Control mice consisted of age-matched littermates with two wild-type (WT) alleles at the *Rhpn2* locus (*Rhpn2*$^{+/+}$). All animal studies were authorized by the Animal Care Use and Review Committee of the Université Libre de Bruxelles.

Genotyping by PCR. Mice were genotyped using genomic tail DNA in a PCR with primers 1 (5′-CTT GTC AGT CTT GCT TGG AAA-3′) and 2 (5′-GGG TTC AAG ACT GTA AGG CGG-3′) for the WT allele and primers 1 and 3 (5′-AGG ACA GCA AGG GGG AGG ATT-3′) for the mutated allele, yielding 370- and 580-bp DNA fragments, respectively.

RNA hybridization and RT-PCR. RNA (RNeasy mini kit; QIAGEN GmbH, Hilden, Germany) was isolated from mouse thyroid, brain, kidney, spleen, liver, testis, ovary, lung, and heart. For RNA hybridization, the probe was either the [α-^{32}P]dATP-radiolabeled dog rhophilin 2 cDNA fragment described above or an actin cDNA fragment. For reverse transcription-PCR (RT-PCR), RNA was reverse transcribed using random hexamer primers, and DNA fragments were amplified with primers P5 (5′-TTT TAT TTT GGA ACA CTA CA-3′, located in exon 5) and P7a (5′-TCT GCC GGT TAC AGC GGG TC-3′, located in exon 7, proximal to the Eco47III restriction site), P5 and P7b (5′-CTG CAG CTC TTT GAA AGG C-3′, located in exon 7, distal to the Eco47III restriction site) and P5 and P8 (5′-GGG CTC ATG TCG TAA CTT G-3′, located in exon 8); hypoxanthine phosphoribosyltransferase served as a standard to balance the amount of mRNA used (primers 5′-GCT GGT GAA AAG GAC CTC T-3′ and 5′-CAC AGG ACT AGA ACA CCT GC-3′).

Western blot analysis. Protein extracts (40 μg/lane) from *Rhpn2*$^{+/+}$ and *Rhpn2*$^{-/-}$ brain samples were separated by sodium dodecyl sulfate-polyacrylamide gel electrophoresis and transferred to a nitrocellulose membrane. The membrane was incubated first in a blocking solution and then with a rabbit polyclonal anti-Rhpn2 antibody (1/500 dilution) (8). After washing, peroxidase-labeled donkey anti-rabbit immunoglobulins were added, and finally, the membrane was incubated with enhanced chemiluminescence reagents and autoradiographed. Protein loading was determined with an anti-actin antibody.

Tests of thyroid function. Thyroidal radioiodide uptake was measured by counting (Packard 2900TR counter) whole thyroid glands 2 days after intraperitoneal injection of 5 μCi of Na^{131}I. Blood samples were obtained by retro-orbital puncture under ether anesthesia. Circulating TSH and T4 hormones were measured in serum samples kept frozen at −70°C. T4 was measured by double antibody precipitation radioimmunoassay (Diagnostic Products, Los Angeles, Calif.) modified to measure T4 in mouse serum with a sensitivity of 0.25 μg/dl. Mouse TSH was measured by a radioimmunoassay (11). The sensitivity of the assay is 5 to 10 mU/liter.

Histological procedures. Tissue samples were fixed in 10% neutral-buffered formalin and embedded in paraffin by standard procedures (1). Sections (6 μm) were stained with hematoxylin and eosin. For thyroid, the area of each follicle was estimated by measuring the smaller inner diameter (d) and the larger inner diameter (D) of the follicle. The approximate follicular lumen area was calculated by the formula $A = \pi(d/2)(D/2)$. More than 100 follicles were measured in each thyroid gland. For each mouse, cell density per square millimeter was estimated by counting the number of cells in 15 areas of 0.0373 mm^2, and follicle density was estimated by counting eight areas of 0.1485 mm^2.

Statistical analysis. Statistical significance was analyzed with an unpaired t test.

RESULTS

Sequence and tissue expression of the mouse *Rhpn2* cDNA. Different results concerning the mouse *Rhpn2* cDNA sequence and gene intron and exon structures have been reported in the National Center for Biotechnology Information (NCBI) and Ensembl databases (Fig. 1A). Indeed, in the NCBI database, the Rhpn2 coding sequence in mouse (accession no. 52428) is 2,058 bp long, as in human (accession no. 85415) and dog (accession no. 403518). The mouse *Rhpn2* locus was localized on chromosome 7 B1 (at 11.0 cM) and was found to be 55.6 kb long and to have 15 exons, as in human. In the Ensembl database, however, only 11 exons were identified on mouse chromosome 7 B1, and they corresponded to the last 11 exons described in the NCBI database (accession no. ENSMUSG00000030494) (data not shown). The first exon of the *Rhpn2* gene reported in the Ensembl database (the equivalent of the fifth exon in the NCBI database) contained an in-frame AUG codon but no favorable context for initiating translation (data not shown). Given the uncertainty about the mouse *Rhpn2* coding sequence, we decided to isolate and analyze the mouse *Rhpn2* cDNA. After screening of a mouse brain cDNA library and amplification of the mouse *Rhpn2* cDNA 5′ end by 5′ RACE, we confirmed the NCBI database results with a 2,058-bp-long coding region, predicting a 686-amino-acid protein, as in human and dog. Expression analysis of Rhpn2 mRNA in various mouse tissues revealed its presence in brain, thyroid, and testis at high levels and in lung, kidney, and ovary at lower levels. No signal was detected in liver, spleen, and heart (Fig. 1B). The presence of a unique signal at ~4.0 kb in RNA hybridization excluded the possibility of abundantly expressed alternative splicing isoforms.

Generation of *Rhpn2*-deficient mice. A targeting vector designed to delete parts of exon 7 and intron 7 of the mouse *Rhpn2* gene was constructed (Fig. 2A). In this vector, the 1-kb deleted genomic DNA fragment was replaced by a 2.3-kb neomycin resistance cassette (Neo). The targeting vector was lin-

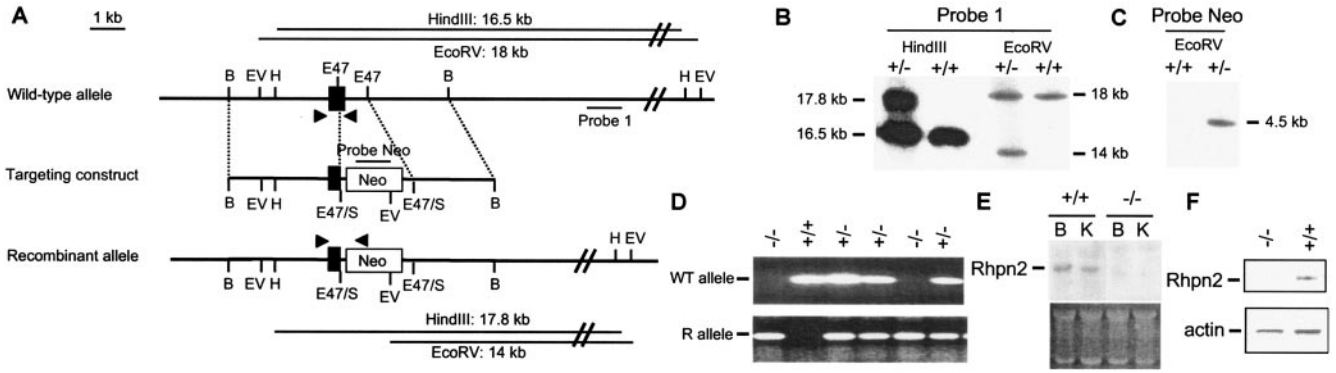

FIG. 2. Targeted disruption of mouse *Rhpn2*. (A) Wild-type allele, targeting vector, predicted structure of the mutant allele, probes used in Southern blot analysis, DNA fragments generated after digestion with HindIII or EcoRV, and primers used for mouse genotyping by PCR (filled arrowheads). Filled boxes: exon 7 of the *Rhpn2* gene. B, BamHI; EV, EcoRV; E47, Eco47III; E47/S, E47 DNA fragment ligated into SmaI-digested vector; H, HindIII. (B and C) Southern blots of the recombinant embryonic stem cell clone with probe 1 and the probe corresponding to the Neo cassette. Left and/or right margins, length of genomic DNA fragments generated after digestion with restriction enzymes (above blot). (D) Mouse genotyping by PCR amplification from tail DNA using primers specific for either the WT or the recombinant (R) allele. (E) RNA hybridization analysis of total brain (B) and kidney (K) RNA isolated from $Rhpn2^{+/+}$ and $Rhpn2^{-/-}$ mice. The probe was a 2.2-kb dog rhophilin 2 cDNA fragment containing the complete coding region. (F) Western blot of brain protein extract from $Rhpn2^{+/+}$ and $Rhpn2^{-/-}$ mice using anti-Rhpn2 or anti-actin antibody.

earized and electroporated in R1 ES cells, which were selected for G418 resistance. One single ES cell clone out of 264 harbored the correct integration of the targeting construct when probed by Southern blotting with a 1-kb DNA fragment located outside the recombination region (Fig. 2B). The single recombination event was confirmed by Southern blotting using a DNA fragment corresponding to the neomycin resistance cassette as a probe: a single 4.5-kb signal was identified, indicating the absence of random integration of the targeting vector in the ES cell genome (Fig. 2C). $Rhpn2^{+/-}$ ES cells were aggregated with CD1 morulae, and 12 chimeric mice were bred with CD1 mice to produce heterozygous mice. The resulting heterozygotes were intercrossed to generate homozygous mice. Genotyping of the progeny revealed that *Rhpn2* null mice were born at the Mendelian frequency (Table 1). Genotyping of the mice was verified by PCR (Fig. 2A and D). $Rhpn2^{-/-}$ mice appeared grossly normal and showed normal body weight (data not shown). Their life spans were normal in comparison with those of their wild-type littermates (data not shown). Both male and female $Rhpn2^{-/-}$ mice were fertile, and they were found to produce litters of normal size (data not shown). The absence of *Rhpn2* mRNA in brain and kidney in the RNA hybridization assay as well as of Rhpn2 protein in brain extract in Western blotting analysis confirmed that the substitution of parts of exon 7 and intron 7 by a neomycin resistance cassette created a null mutation (Fig. 2E and F).

TABLE 1. Genotype analysis of progeny resulting from crosses of $Rhpn2^{+/-}$ mice

Mouse group	No. of mice with indicated genotype (% of total)			No. of mice (% of total)
	+/+	+/−	−/−	
Female	12	30	14	56 (49.1)
Male	14	25	19	58 (50.8)
Total	26 (22.8)	55 (48.2)	33 (28.9)	114

Normal thyroid function and histology in $Rhpn2^{-/-}$ mice. The absence of normal *Rhpn2* mRNA in the thyroid of $Rhpn2^{-/-}$ mice was verified by RT-PCR: total RNA was isolated from $Rhpn2^{+/+}$ and $Rhpn2^{-/-}$ thyroids, reverse transcribed with random hexamer primers, and PCR amplified with the specific primers depicted in Fig. 3A. In both $Rhpn2^{+/+}$ and $Rhpn2^{-/-}$ mice, a 319-bp DNA fragment was amplified with primers P5 and P7a, located in exon 5 and 7, respectively (Fig. 3A and B). However, with primers P5 and P7b (located downstream of the neomycin resistance cassette) as well as with primers P5 and P8 (located in exon 8), DNA fragments of the expected size were only obtained in $Rhpn2^{+/+}$ thyroid.

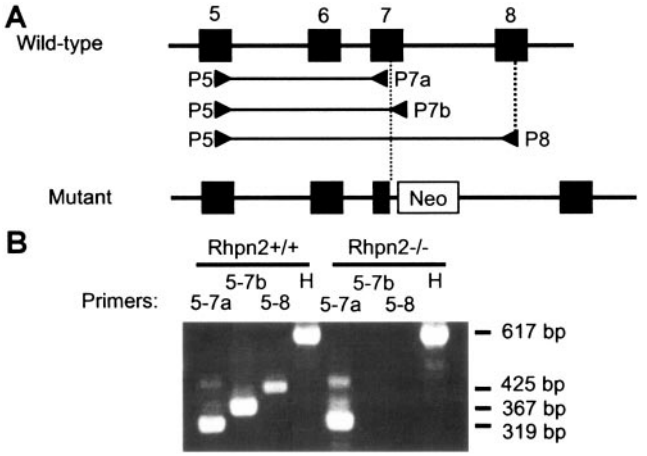

FIG. 3. Absence of normal *Rhpn2* mRNA in $Rhpn2^{-/-}$ thyroid. (A) Exons 5 to 8 (filled boxes) of the mouse *Rhpn2* gene in wild-type and mutant alleles and localization of primers P5, P7a, P7b, and P8 (arrowheads). (B) Electrophoresis of PCR products generated with the indicated primers on cDNA isolated from $Rhpn2^{+/+}$ and $Rhpn2^{-/-}$ thyroids. H, hypoxanthine phosphoribosyltransferase primers. Right margin, lengths of DNA fragments generated by PCR.

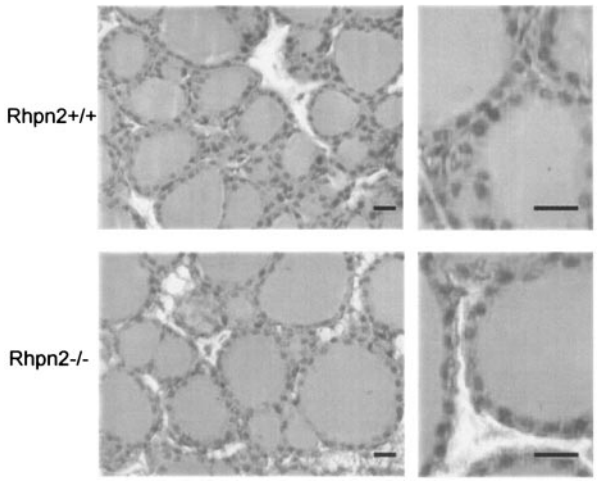

FIG. 4. Normal histological structure of *Rhpn2*$^{-/-}$ thyroid. Thyroid lobes and follicles from *Rhpn2*$^{+/+}$ and *Rhpn2*$^{-/-}$ mice are shown (scale bar, 15 μm).

These results confirm the absence of normal *Rhpn2* mRNA in the thyroid of our knockout mice (Fig. 3).

Rhpn2$^{-/-}$ mice had no visible goiter and no obvious signs of hyper- or hypothyroidism; they had normal body weight and normal behavioral activity, two characteristics that are expected to be impaired in severe thyroid disease.

Cross-section and hematoxylin and eosin staining of 11-week-old *Rhpn2*$^{+/+}$ and *Rhpn2*$^{-/-}$ thyroid gland samples revealed no abnormalities in follicular structure; the morphology of cells was also perfectly normal (Fig. 4). The absence of Rhpn2 in thyroid gland did not induce visible hyperplasia, and no signs of tumor induction were seen. In *Rhpn2*$^{-/-}$ mice, the number of cells and follicles per square millimeter were in the normal range, and follicle size was not significantly different from that of *Rhpn2*$^{+/+}$ mice (Fig. 5A, B, and C). Furthermore, thyroidal radioiodide uptake was measured 2 days after intraperitoneal injection of 5 μCi of $Na^{131}I$ in control and knockout mice. There was no significant difference in radioiodide uptake

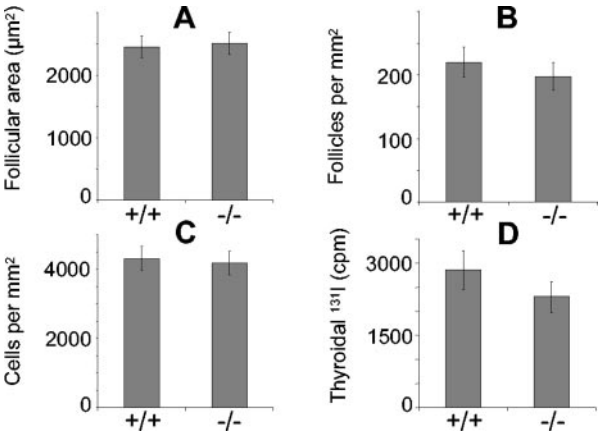

FIG. 5. Morphological parameters measured in thyroid glands of *Rhpn2*$^{+/+}$ and *Rhpn2*$^{-/-}$ mice. (A) Average follicular area. (B) Follicular density. (C) Cellular density. (D) Thyroidal ^{131}I uptake 2 days after injection of the isotope. Values are means ± standard errors of the means (five mice per group).

TABLE 2. Serum T4 and TSH levels in *Rhpn2*$^{+/+}$ and *Rhpn2*$^{-/-}$ mice[a]

Hormone	Hormone level (mean ± SD) in indicated mouse group (no. of mice)		P^b
	+/+	−/−	
T4 (ng/ml)	40 ± 14 (8)	44 ± 11 (8)	0.928
TSH (mU/liter)	78 ± 30 (8)	76 ± 54 (8)	0.496

[a] SD, standard deviation.
[b] As determined by *t* testing.

by *Rhpn2*$^{+/+}$ and *Rhpn2*$^{-/-}$ thyroids (Fig. 5D). In order to investigate the regulation of thyroid hormone synthesis, serum T4 and TSH levels were analyzed in 8-week-old control and mutant mice. Serum T4 in *Rhpn2*$^{-/-}$ mice was not significantly different from that in control mice, and the same levels of TSH, the most sensitive indicator of thyroid function, were observed in *Rhpn2*$^{+/+}$ and *Rhpn2*$^{-/-}$ mice (Table 2).

Normal brain, lung, ovary, testis, and kidney histological structure in *Rhpn2*-deficient mice. Since besides thyroid, Rhpn2 is significantly expressed in brain, lung, ovary, testis, and kidney, these organs were carefully examined in *Rhpn2*$^{-/-}$ mice for the presence of histological alterations (Fig. 6). Histological analysis indicated that all these organs in *Rhpn2* null mice appeared to be similar to those in wild-type mice. For example, the size and structure of the hippocampus (Fig. 6), cerebral cortex, and cerebellum (data not shown) at low and high magnifications appeared normal in the mutant mice. In the *Rhpn2*$^{-/-}$ lung, a normal bronchial tree, from the bronchioles to the alveoli, was observed (Fig. 6). In particular, the interalveolar septum, the respiratory bronchioles, and the branches of the pulmonary arteries appeared normal in the mutant mice (Fig. 6). The histological structures of the ovaries in *Rhpn2*$^{+/+}$ and *Rhpn2*$^{-/-}$ mice were indistinguishable (Fig. 6). In *Rhpn2*$^{-/-}$ ovary, the cortex and the medulla were normal, and the presence of follicles at different stages of differentiation was observed. In the testis, no obvious alteration was detected: the interstitial cells and the seminiferous tubules were normal (Fig. 6). All the differentiation stages of spermatogenesis, from the primitive germ cells—the spermatogonium—to the spermatozoa, were observed. The histological structure of the kidney was also similar in *Rhpn2*$^{+/+}$ and *Rhpn2*$^{-/-}$ mice (Fig. 6). A normal renal capsule, cortex, and medulla were detected in the mutant mice, and normal glomeruli, tubules, and arterioles were observed (Fig. 6).

DISCUSSION

In order to identify new genes whose expression in the thyroid is positively or negatively modulated by chronic TSH stimulation, a differential screening of a methimazole- and propylthiouracil-treated dog thyroid cDNA library was previously performed using cDNA probes isolated from either quiescent or TSH-stimulated thyroid tissues (17). Among 19 genes identified in the differential screening, *Rhpn2* was estimated to be a good candidate for a potential important functional role in the thyroid in response to the differentiation hormone TSH for the following reasons: Rhpn2 is expressed in the thyroid (8, 17); its expression at the mRNA and protein levels in primary

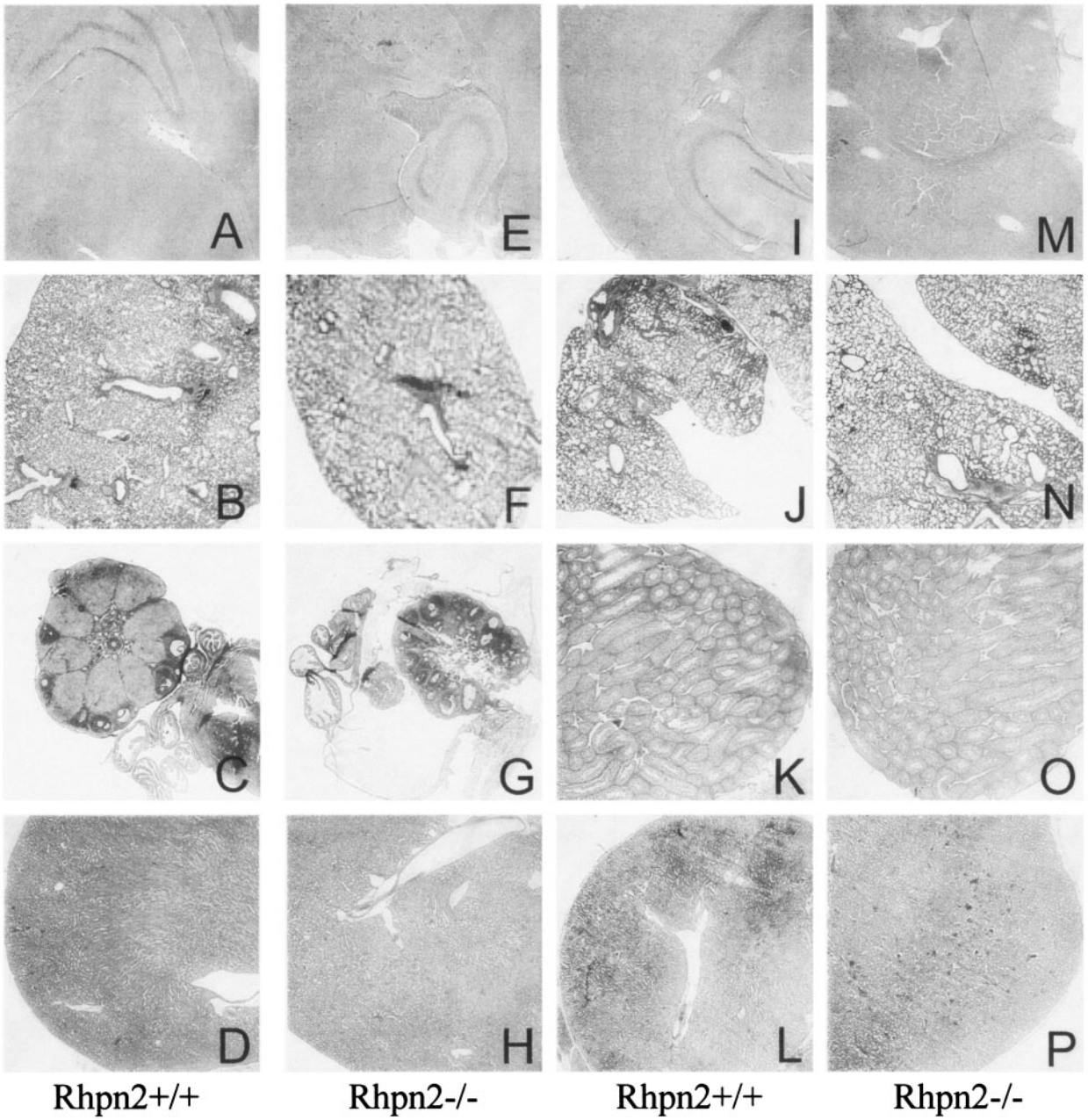

FIG. 6. Normal histological structure of brain, lung, ovary, testis, and kidney in *Rhpn2*$^{-/-}$ mice: hematoxylin and eosin-stained sections from brain (A, E, I, and M), lung (B, F, J, and N), ovary (C and G), testis (K and O), and kidney (D, H, L, and P) of 12-week-old *Rhpn2*$^{+/+}$ (first and third columns) and *Rhpn2*$^{-/-}$ (second and fourth columns) mice. Low-magnification pictures are shown.

dog thyrocyte culture is increased in response to TSH after 4 to 6 and 6 to 8 h, respectively (8); activation of the tyrosine kinase/mitogen-activated protein kinase pathway by growth factors like epidermal growth factor and hepatocyte growth factor, or of the phorbol ester/protein kinase C pathway by 4β-phorbol 12-myristate 13-acetate—all dedifferentiation factors of thyroid cells—did not increase Rhpn2 mRNA expression in dog thyrocyte primary culture (8); and Rhpn2 binds in vitro to the activated form of RhoB, a small GTPase which regulates actin cytoskeleton rearrangements, as well as to components of the cytoskeleton (8). *Rhpn2* thus seems to behave as a immediate-early gene of the cyclic AMP/TSH differentiation cascade in the thyroid cell. It was suggested to play a potential role in the control of intracellular motile phenomena, such as the endocytosis involved during the thyroid secretory process. This hypothesis seemed plausible, because of the known role of Rho GTPases and Rho effectors in the regulation of actin cytoskeleton, membrane trafficking and secretion, cell growth, gene expression, and cytokinesis (6). For exemple, inactivation of the Rho effector citron kinase in mice confirmed its role in the control of cytokinesis: citron kinase-deficient mice are ataxic and die prematurely from seizures (2). In these mice, altered cytokinesis and massive apoptosis were shown to be responsible for defective neurogenesis, which includes deple-

tion of specific neuronal populations. The formin mDia, another Rho effector and the mammalian homolog of *Drosophila* diaphanous, has recently been implicated in microtubule stabilization via the formation of complex with EB1 and adenomatous polyposis coli at stable microtubule ends (16). PRK1 and PRK2, two members of the protein kinase C-related protein kinase family, are involved in the control of mitogenesis, apoptosis, and cell adhesion. Surprisingly, the analysis of ROCK-II-deficient mice failed to confirm the direct implication of this Rho effector in the reorganization of actin cytoskeleton (15). Indeed, most ROCK-II$^{-/-}$ mice die in utero from severely decreased fibrinolytic activity causing the formation of large thrombus in the labyrinth of the placenta, without affecting F-actin structure or stress fiber formation. Finally, it has recently been shown that CNK1, a new Rho effector acting as a scaffold protein linking Rho and Ras signal transduction pathways, associates with rhophilin (7). Given the importance of both pathways in cancer cells, it is of particular importance to look at a potential role of rhophilin in the process of cell proliferation and transformation.

In order to validate our hypotheses concerning the potential role of Rhpn2 in thyroid cell physiology in vivo, Rhpn2-deficient mice were produced. As a first step in the construction of the targeting vector, a mouse genomic DNA fragment containing an exon of the *Rhpn2* gene was isolated. To our surprise, the comparison of our exon 7-containing genomic DNA fragment of the mouse *Rhpn2* gene with data available in the NCBI and Ensembl databases revealed a discrepancy in the number of exons in the gene as well as in the length of the coding region of its cDNA. Cloning and sequencing of the coding region of the Rhpn2 cDNA in mouse confirmed that it is 2,058 bp long, as in dog and human, and as more recently described by Peck et al. (10).

Rhpn2-deficient mice showed no major morphological abnormalities, had normal body weights, behavioral activities, and life spans, and were fertile, suggesting no major thyroid dysfunction. The microscopic structures of the thyroid, brain, testis, ovary, kidney, and lung were also normal, and the absence of major thyroid dysfunction was confirmed in various tests, including dosage of serum TSH levels, the most sensitive indicator of thyroid dysfunction.

At the present time, the possible explanations for the absence of detectable thyroid abnormalities in Rhpn2-deficient mice are the following. First, we cannot exclude the possibility that thyroid alterations are too subtle to be detected in Rhpn2$^{-/-}$ mice under normal conditions of life in our animal room or on the genetic background tested. Second, the most widely cited explanation for the absence of major alterations in knockout mice is functional redundancy. Rhpn2 is highly similar to rhophilin 1 (Rhpn1): comparison between mouse Rhpn2 and Rhpn1 revealed that they are similar in size and have three domains in common: the Rho-binding motif at the amino terminus, a central Bro1-like domain of ~200 amino acids, and a carboxy-terminal PDZ domain of limited homology (8, 10). Rhpn1 is expressed in all tissues examined, and seems to be present in the thyroid, as is Rhpn2 (9, 14). The future development of Rhpn1-deficient mice and Rhpn1/Rhpn2 double-knockout mice will be important for determining whether these two Rho-binding proteins have functionally redundant roles. Third, the lack of detectable abnormalities in our Rhpn2 knockout mice might be due to species differences in the relative importance of Rhpn2 in the regulation of thyroid function. Indeed, the functional screening that initially identified the *Rhpn2* gene was performed in dogs, not in mice.

Finally, Rhpn2 is not expressed exclusively in the thyroid, as revealed by RNA hybridization (8, 10) and microarray analysis (14). Besides thyroid, Rhpn2 mRNA has also been detected in the brain, testis, ovary, lung, kidney, prostate, trachea, stomach, colon, mammary gland, salivary gland, and pancreas (8, 10, 14). The possibility that other organ systems might be affected by the absence of Rhpn2 exists. The availability of Rhpn2-deficient mice should also help us to define the physiological role of Rhpn2 in these specific organs.

ACKNOWLEDGMENTS

We thank S. Refetoff (University of Chicago) for TSH and T4 hormone measurements, I. Pirson (Université Libre de Bruxelles) for anti-Rhpn2 polyclonal antibody, and A. Nagy for R1 ES cells.

This work was supported by an EU Biomed 2 grant to J.E.D., the Fonds de la Recherche Scientifique Médicale de Belgique and the Belgian Program on Interuniversity Poles of Attraction initiated by the Belgian State, Prime Minister's office, Federal Service for Science, Technology, and Culture. J.B. was supported by Deutsche Forschungsgemeinschaft grant BE 2156. S.C. and S.S. are, respectively, postdoctoral researcher and research director of the Belgian Fonds National de la Recherche Scientifique.

REFERENCES

1. **Clement, S., S. Refetoff, B. Robaye, J. E. Dumont, and S. Schurmans.** 2001. Low TSH requirement and goiter in transgenic mice overexpressing IGF-I and IGF-Ir receptor in the thyroid gland. Endocrinology **142:**5131–5139.
2. **Di Cunto, F., S. Imarisio, E. Hirsch, V. Broccoli, A. Bulfone, A. Migheli, C. Atzori, E. Turco, R. Triolo, G. P. Dotto, L. Silengo, and F. Altruda.** 2000. Defective neurogenesis in citron kinase knockout mice by altered cytokinesis and massive apoptosis. Neuron **28:**115–127.
3. **Dremier, S., K. Coulonval, S. Perpete, F. Vandeput, N. Fortemaison, A. Van Keymeulen, S. Deleu, C. Ledent, S. Clement, S. Schurmans, J. E. Dumont, F. Lamy, P. P. Roger, and C. Maenhaut.** 2002. The role of cyclic AMP and its effect on protein kinase A in the mitogenic action of thyrotropin on the thyroid cell. Ann. N. Y. Acad. Sci. **968:**106–121.
4. **Dumont, J. E., F. Lamy, P. Roger, and C. Maenhaut.** 1992. Physiological and pathological regulation of thyroid cell proliferation and differentiation by thyrotropin and other factors. Physiol. Rev. **72:**667–697.
5. **Dumont, J. E., C. Maenhaut, F. Lamy, I. Pirson, S. Clement, and P. P. Roger.** 2003. Growth and proliferation of the thyroid cell in normal physiology and in disease. Ann. Endocrinol. **64:**10–11.
6. **Hall, A.** 1998. Rho GTPases and the actin cytoskeleton. Science **279:**509–514.
7. **Jeffe, A. B., P. AspenStröm, and A. Hall.** 2004. Human CNK1 acts as a scoffold protein, linking Rho and Ras signal transduction pathways. Mol. Cell. Biol. **24:**1736–1746.
8. **Mircescu, H., S. Steuve, V. Savonet, C. Degraef, H. Mellor, J. E. Dumont, C. Maenhaut, and I. Pirson.** 2002. Identification and characterization of a novel activated RhoB binding protein containing a PDZ domain whose expression is specifically modulated in thyroid cells by cAMP. Eur. J. Biochem. **269:** 6241–6249.
9. **Nakamura, K., A. Fujita, T. Murata, G. Watanabe, C. Mori, J. Fujita, N. Watanabe, T. Ishizaki, O. Yoshida, and S. Narumiya.** 1999. Rhophilin, a small GTPase Rho-binding protein, is abundantly expressed in the mouse testis and localized in the principal piece of the sperm tail. FEBS Lett. **445:** 9–13.
10. **Peck, J. W., M. Oberst, K. B. Bouker, E. Bowden, and P. D. Burbelo.** 2002. The RhoA-binding protein, rhophilin-2, regulates actin cytoskeleton organization. J. Biol. Chem. **277:**43924–43932.
11. **Pohlenz, J., A. Maqueem, K. Cua, R. E. Weiss, J. Van Sande, and S. Refetoff.** 1999. Improved radioimmunoassay for measurement of mouse thyrotropin in serum: strain differences in thyrotropin concentration and thyrotroph sensitivity to thyroid hormone. Thyroid **9:**1265–1271.
12. **Pouillon, V., R. Hascakova-Bartova, B. Pajak, E. Adam, F. Bex, V. Dewaste, C. Van Lint, O. Leo, C. Erneux, and S. Schurmans.** 2003. Inositol 1,3,4,5-tetrakisphosphate is essential for T lymphocyte development. Nat. Immunol. **4:**1136–1143.
13. **Roger, P. P., D. Christophe, J. E. Dumont, and I. Pirson.** 1997. The dog thyroid primary culture system: a model of the regulation of function, growth and differentiation expression by cAMP and other well-defined signaling cascades. Eur. J. Endocrinol. **137:**579–598.

14. **Su, A. I., T. Wiltshire, S. Batalov, H. Lapp, K. A. Ching, D. Block, J. Zhang, R. Soden, M. Hayakawa, G. Kreiman, M. P. Cooke, J. R. Walker, and J. B. Hogenesch.** 2004. A gene atlas of the mouse and human protein-encoding transcriptomes. Proc. Natl. Acad. Sci. USA **101:**6062–6067.
15. **Thumkeo, D., J. Keel, T. Ishizaki, M. Hirose, K. Nonomura, H. Oshima, M. Oshima, M. M. Taketo, and S. Narumiya.** 2003. Targeted disruption of the mouse Rho-associated kinase 2 gene results in intrauterine growth retardation and fetal death. Mol. Cell. Biol. **23:**5043–5055.
16. **Wen, Y., C. H. Eng, J. Schmoranzer, N. Cabrera-Poch, E. J. Morris, M. Chen, B. J. Wallar, A. S. Alberts, and G. G. Gundersen.** 2004. EB1 and APC bind to mDia to stabilize microtubules downstream of Rho and promote cell migration. Nat. Cell Biol. **6:**820–830.
17. **Wilkin, F., V. Savonet, A. Radulescu, J. Petermans, J. E. Dumont, and C. Maenhaut.** 1996. Identification and characterization of novel genes modulated in the thyroid of dogs treated with methimazole and propylthiouracil. J. Biol. Chem. **271:**28451–28457.